

Parity doublet model for baryon octets: Ground states saturated by good diquarks and the role of bad diquarks for excited states

Bikai Gao^{1,*}, Toru Kojo^{2,†} and Masayasu Harada^{3,1,4,‡}

¹*Department of Physics, Nagoya University, Nagoya 464-8602, Japan*

²*Department of Physics, Tohoku University, Sendai 980-8578, Japan*

³*Kobayashi-Maskawa Institute for the Origin of Particles and the Universe, Nagoya University, Nagoya 464-8602, Japan*

⁴*Advanced Science Research Center, Japan Atomic Energy Agency, Tokai 319-1195, Japan*



(Received 1 April 2024; accepted 14 June 2024; published 18 July 2024)

Parity doublet model is an effective chiral model that includes the chiral-variant and -invariant masses of baryons. The chiral-invariant mass has large impacts on the density dependence of models which can be constrained by neutron star observations. In the previous work, models of two flavors have been considered up to a few times nuclear saturation density, but in such dense regions it is also necessary to consider hyperons. With the chiral-invariant masses baryons can stay massive in extreme environments (e.g., neutron stars) where the chiral symmetry restoration takes place. In this work, we generalize the previous $SU(2)_L \times SU(2)_R$ parity models of nucleons to $SU(3)_L \times SU(3)_R$ models of the baryon octet within the linear realization of the chiral symmetry. The major problem in constructing such models has been too many candidates for the chiral representations of baryons. Motivated by the concepts of diquarks and the mended symmetry, we choose the $(3_L, \bar{3}_R) + (\bar{3}_L, 3_R)$, $(3_L, 6_R) + (6_L, 3_R)$, and $(1_L, 8_R) + (8_L, 1_R)$ representations and use quark diagrams to constrain the possible types of Yukawa interactions. The masses of the baryon octets for positive and negative baryons up to the first excitations are successfully reproduced. As expected from the diquark considerations, the ground-state baryons are well dominated by $(3_L, \bar{3}_R) + (\bar{3}_L, 3_R)$ and $(1_L, 8_R) + (8_L, 1_R)$ representations, while the excited states require $(3_L, 6_R) + (6_L, 3_R)$ representations. Important applications of our model are the chiral restoration for strange quarks at large density and the continuity of diquarks from hadronic to quark matter. We also address the problem of large Yukawa couplings which are enhanced in three-flavor construction.

DOI: [10.1103/PhysRevD.110.016016](https://doi.org/10.1103/PhysRevD.110.016016)

I. INTRODUCTION

Understanding of the origin of the nucleon mass is one of the most fundamental subjects in hadron physics. Traditionally, the chiral symmetry in quantum chromodynamics (QCD) and its spontaneous symmetry breaking (SSB) [1–4] are often used to study the nucleon mass. The order parameter of the SSB is the chiral condensate $\langle \bar{q}q \rangle$, which is made of quark-antiquark pairs with different chirality [5–7]. The existence of chiral condensate breaks the chiral symmetry because it couples quarks of different chirality, and in vacuum it has a nonzero value.

In certain extreme conditions, such as high-density or high-temperature regions, the chiral condensate may vanish with the restoration of chiral symmetry in the thermodynamic state.

The linear sigma model (LSM) is an effective model broadly used for investigating the SSB. In the LSM, the order parameter of SSB is the expectation values of the scalar field $\langle \sigma \rangle \propto \langle \bar{q}q \rangle$. In the traditional hadronic model with the LSM, the nucleon mass m_N is considered to be generated mainly by chiral condensates. An interesting consequence of this perspective is that the nucleon mass vanishes in the high-density or high-temperature region where the chiral symmetry should be restored.

However, the traditional view of nucleon masses being completely originated from the chiral condensate is being reconsidered due to the insights gained from lattice QCD simulations [8–12]. These lattice QCD results have indicated the possibility of a chiral-invariant mass, denoted as m_0 , which seems to exist apart from the conventional chiral-variant mass which has dependence over the density or temperature. This novel concept of a chiral-invariant

*Contact author: gaobikai@hken.phys.nagoya-u.ac.jp

†Contact author: torujj@nucl.phys.tohoku.ac.jp

‡Contact author: harada@hken.phys.nagoya-u.ac.jp

Published by the American Physical Society under the terms of the [Creative Commons Attribution 4.0 International license](https://creativecommons.org/licenses/by/4.0/). Further distribution of this work must maintain attribution to the author(s) and the published article's title, journal citation, and DOI. Funded by SCOAP³.

mass suggests that the nucleon mass would keep a finite value even when the chiral symmetry is restored. The concept of the chiral-invariant mass is naturally incorporated in a parity doublet model (PDM) for nucleons in which the ordinary nucleon and its parity partner form a doublet structure [13–20]. Within this framework, nucleon masses in the PDM are found to be less sensitive to the chiral condensate than in the conventional LSM. This changing of the sensitivity has far-reaching consequences, especially when we construct the equation of state (EOS) for nuclear and neutron star (NS) matter. The introduction of chiral-invariant mass leads to significant changes in the coupling constants, which, in turn, greatly affect the stiffness of the EOS.

In the context of applications to NS phenomenology, the nuclear EOS within the PDM is often extended to densities beyond the nuclear saturation density n_0 [21,22]. This extrapolation has been achieved in various ways. One approach involves a straightforward extrapolation of the PDM EOS beyond $n_0 \simeq 0.16 \text{ fm}^{-3}$, as studied in Ref. [23]. Another method combines the PDM EOS with a quark model, assuming a quark-hadron crossover, which allows for a smooth transition from hadronic matter to quark matter [24–29]. This hybrid approach, where the PDM EOS is employed up to densities around $2n_0$ to $3n_0$ and interpolate with the quark EOS at $\geq 5n_0$ via polynomial interpolants to obtain the unified EOS. This unified EOS is valuable for modeling the behavior of dense matter within neutron stars and can provide us with important insights into the intermediate density region. However, the validity of a purely hadronic picture at densities above $2n_0$ is questionable because hyperons, strange baryons containing strange quarks, may enter the matter and affect its properties. Taking this possibility into consideration, it becomes necessary to explore the effect of a strange quark in the finite density region. In a previous study of the nuclear matter domain, we included the strange quark effects through the Kobayashi–Maskawa–’t Hooft interactions and constructed a three-flavor mesonic Lagrangian made of scalar and vector mesons [27]. The corresponding unified EOS was confronted with NS constraints from the NS merger GW170817 [30–32], the millisecond pulsar PSR J0030 + 0451 [33], and the maximum mass constraint from the millisecond pulsar PSR J0740 + 6620 [34]. Based on the above NS observation data, we constrained m_0 to the range $400 \text{ MeV} \lesssim m_0 \lesssim 700 \text{ MeV}$, which is more relaxed than the one obtained in Ref. [25].

In the analyses in Refs. [25–28], we assumed that the hyperons do not appear in the density region below $2n_0$. On the other hand, the analysis in Ref. [26] shows that strangeness number density starts to appear in the crossover region at $n_B \gtrsim 2n_0$. This indicates that the hyperons might appear even below $2n_0$. To clarify this, we need to construct a parity doublet model including hyperons. There

were several analyses of chiral models with the parity doublet structure based on the $SU(3)_L \otimes SU(3)_R$ chiral symmetry [35–43]. Since the $SU(3)$ -flavor-octet baryons appear from the chiral representation of $(3_L, \bar{3}_R)$, $(8_L, 1_R)$, $(3_L, 6_R)$ with $L \leftrightarrow R$; all three chiral representations are included in most of these analyses.

In the previous analysis [40], we adopted the dynamical assumption and included only $(3_L, \bar{3}_R)$ and $(8_L, 1_R)$ (and $L \leftrightarrow R$) representations which are made from the so-called good diquark without including $(3_L, 6_R)$ (and $L \leftrightarrow R$) from the “bad diquark.” Based on the quark diagrams, we constructed Yukawa interactions of baryons to the chiral field Σ , the vacuum expectation value (VEV) of which spontaneously breaks the chiral symmetry. Then, we have proven that the first-order interactions cannot reproduce the correct mass ordering of octet baryons in the ground state, $m_N < m_\Lambda \sim m_\Sigma < m_\Xi$. We also showed that the inclusion of the second-order Yukawa interactions can generate the correct mass ordering of the ground-state baryons. However, in the excited states, the mass ordering appears to be incorrect for the wide domain of model parameters which we have exhaustively explored. This indicates that models made only of baryons with good diquarks, even after including the Yukawa interactions up to the second order, misses some qualitative features of the baryon spectra.

In the present analysis, we include the $(3_L, \bar{3}_R)$, $(8_L, 1_R)$, and $(3_L, 6_R)$ (and $L \leftrightarrow R$) chiral representations and construct the Yukawa interactions based on the quark diagram as in Ref. [40]. We will show that the mass ordering of the excited states is correctly reproduced within the reasonable range of parameters; the problem found in Ref. [40] is solved. Furthermore, we study the composition of chiral representations in the ground and excited baryons. We found that the ground states are dominated by the representations of $(3_L, \bar{3}_R)$ and $(8_L, 1_R)$ made of good diquarks. This finding is consistent with the conventional arguments in the hadron spectroscopy. Meanwhile, the excited baryons contain the substantial component of $(3_L, 6_R)$ with bad diquarks. This finding is rather new; discussions on bad diquarks in our paper should not be confused with the mass splitting between the baryon octet and decuplet (e.g., the $N - \Delta$ splitting), for which diquarks offer simple explanations. Instead, our work addresses diquarks for the mass splitting between the ground and excited states *within* the baryon octet; here the utility of diquarks has not been established.

This paper is structured as follows. In Sec. II, the chiral representations of $(3_L, \bar{3}_R) + (\bar{3}_L, 3_R)$, $(3_L, 6_R) + (6_L, 3_R)$, and $(8_L, 1_R) + (1_L, 8_R)$ for octet baryons are defined. In Sec. III, we construct an effective Lagrangian for baryons including first-order Yukawa interactions. In Sec. IV, we perform numerical fit of baryon spectra. Section V is devoted to the summary.

II. MODEL CONSTRUCTION

In the chiral $SU(3)_L \times SU(3)_R$ symmetry, there are so many chiral representations for baryons. To keep only a minimal set of necessary fields, we first consider the quark substructure for each representation and then choose baryon fields which are supposed to be relevant from low to intermediate energies. We further include the parity doublet structure to consider the chiral-invariant mass.

The chiral representations of quarks under chiral $SU(3)_L \times SU(3)_R$ symmetry are written as

$$(q_L)^l \sim (3_L, 1_R) \sim (u_L, d_L, s_L)^l, \quad (1)$$

$$(q_R)^r \sim (1_L, 3_R) \sim (u_R, d_R, s_R)^r, \quad (2)$$

where the indices $l = 1, 2, 3$ and $r = 1, 2, 3$ are for $SU(3)_L$ and $SU(3)_R$ symmetries, respectively. Since a baryon can be expressed as a direct product of three quarks, the possible combinations are $(q_L)^3$, $(q_L)^2 q_R$, $q_L (q_R)^2$, and q_R^3 . It is sufficient to consider the following possibilities for the chiral representations of baryons:

$$\begin{aligned} & q_L \times (q_L \times q_L + q_R \times q_R) \\ & \sim (1_L, 1_R) + (8_L, 1_R) + (8_L, 1_R) \\ & \quad + (10_L, 1_R) + (3_L, \bar{3}_R) + (3_L, 6_R) \end{aligned} \quad (3)$$

and $L \leftrightarrow R$. The octet baryons are included in $(3_L, \bar{3}_R)$, $(8_L, 1_R)$, and $(3_L, 6_R)$, which are illustrated in Fig. 1. Following Ref. [38], in the framework of the parity doublet model we introduce the corresponding baryon fields ψ , χ , and η and its parity doubling partners ψ^{mir} , χ^{mir} , and η^{mir} as

$$\psi_L \sim (3_L, \bar{3}_R), \quad \psi_L^{\text{mir}} \sim (\bar{3}_L, 3_R), \quad (4)$$

$$\chi_L \sim (8_L, 1_R), \quad \chi_L^{\text{mir}} \sim (1_L, 8_R), \quad (5)$$

$$\eta_L \sim (3_L, 6_R), \quad \eta_L^{\text{mir}} \sim (6_L, 3_R). \quad (6)$$

Here the indices L and R in the subscripts of ψ , χ , and η represents the chirality in $U(1)_A$, e.g., $\gamma_5 \psi_{R,L} = \pm \psi_{R,L}$. The right-handed fields are also defined in the similar way. Under the parity transformation (\mathcal{P}) and the charge

conjugation (\mathcal{C}), these fields transform as

$$\begin{aligned} \Psi_{l,r} &\xrightarrow{\mathcal{P}} \gamma_0 \Psi_{r,l}, & \Psi_{l,r}^{\text{mir}} &\xrightarrow{\mathcal{P}} -\gamma_0 \Psi_{r,l}^{\text{mir}}, \\ \Psi_{l,r} &\xrightarrow{\mathcal{C}} C(\bar{\Psi}_{r,l})^T, & \Psi_{l,r}^{\text{mir}} &\xrightarrow{\mathcal{C}} -C(\bar{\Psi}_{r,l}^{\text{mir}})^T, \end{aligned} \quad (7)$$

for $\Psi = \psi, \chi, \eta$ with $C = i\gamma^2\gamma^0$. This assignment for the parity is called the mirror assignment.

The irreducible representations of chiral $SU(3)_L \times SU(3)_R$, ψ , χ , and η , are not generally irreducible representations of the flavor $SU(3)_{V=L+R}$. Here we briefly look at how ψ , χ , and η can be expressed in terms of the conventional flavor $SU(3)_V$, as we will eventually consider the chiral SSB, $SU(3)_L \times SU(3)_R \rightarrow SU(3)_V$.

The field $\psi_L \sim (3_L, \bar{3}_R)$ can be written as

$$(\psi_L)_a^{\bar{a}} = \frac{\delta_a^{\bar{a}}}{\sqrt{3}} \Lambda_{0L} + (B_{\psi L})_{\bar{a}}^a, \quad (8)$$

where $a = 1, 2, 3$ are for the fundamental representations in $SU(3)_L$ and $\bar{a} = 1, 2, 3$ for the antifundamental representations in the $SU(3)_R$. The Λ_0 is the flavor singlet Λ , while B is the flavor octet

$$B_\psi = \begin{pmatrix} \frac{1}{\sqrt{2}}\Sigma^0 + \frac{1}{\sqrt{6}}\Lambda & \Sigma^+ & p \\ \Sigma^- & \frac{-1}{\sqrt{2}}\Sigma^0 + \frac{1}{\sqrt{6}}\Lambda & n \\ \Xi^- & \Xi^0 & \frac{-2}{\sqrt{6}}\Lambda \end{pmatrix}_\psi. \quad (9)$$

We can repeat similar assignments for $\chi_L \sim (8_L, 1_R)$,

$$(\chi_L)_b^a = (B_{\chi L})_b^a, \quad (10)$$

where B_χ has the same matrix structure as B_ψ . The indices $\bar{b} = 1, \dots, 3$ represents $\bar{3}_L$. We note that B_ψ and B_χ transform differently in $SU(3)_L \times SU(3)_R$ but show the same transformation under the flavor $SU(3)_V$; in models having only the $SU(3)_V$ symmetry, they are degenerate. Finally, the field $\eta_L \sim (3_L, 6_R)$ can be labeled as

$$(\eta_L)^{(a,\alpha\beta)} = \frac{1}{\sqrt{6}} (e^{a\alpha\gamma} \delta_b^\beta + e^{b\alpha\gamma} \delta_b^\alpha) (B_{\eta L})_b^\gamma, \quad (11)$$

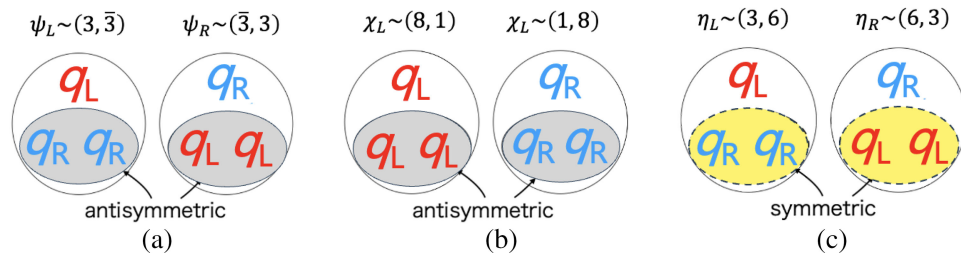


FIG. 1. Quark contents for three baryon representations: (a) $(3_L, \bar{3}_R) + (\bar{3}_L, 3_R)$, (b) $(8_L, 1_R) + (1_L, 8_R)$, and (c) $(3_L, 6_R) + (6_L, 3_R)$. The gray shaded diquark indicates the flavor-antisymmetric representation, while the yellow shaded area indicates the symmetric one.

with B_η having the same structure as $B_{\psi,\chi}$. We can write the right-handed fields in the same way.

For mirror fields, we just exchange the index for the $U(1)_A$ to get the same assignment rules. For example, the field $\psi_R^{\text{mir}} \sim (3_L, \bar{3}_R)$ can be written as

$$(\psi_R^{\text{mir}})_\alpha^a = \frac{\delta_\alpha^a}{\sqrt{3}} \Lambda_{0R} + (B_{\psi_R^{\text{mir}}})_\alpha^a. \quad (12)$$

We list chiral transformation properties for the ψ , η , and χ fields as

$$\psi_L \rightarrow g_L \psi_L g_R^\dagger, \quad \psi_R \rightarrow g_R \psi_R g_L^\dagger, \quad (13)$$

$$\eta_L \rightarrow g_L \eta_L g_R^\dagger, \quad \eta_R \rightarrow g_R \eta_R g_L^\dagger, \quad (14)$$

$$\chi_L \rightarrow g_L \chi_L g_R^\dagger, \quad \chi_R \rightarrow g_R \chi_R g_L^\dagger. \quad (15)$$

In the mirror assignment, the fields ψ_L and ψ_R^{mir} follow the same transformation under the $SU(3)_L \times SU(3)_R$, i.e., $\psi_L \rightarrow g_L \psi_L g_R^\dagger$ and $\psi_R^{\text{mir}} \rightarrow g_L \psi_R^{\text{mir}} g_R^\dagger$. This allows the mass term $\text{tr}[\bar{\psi}_L \psi_R^{\text{mir}}]$, which is invariant under $SU(3)_L \times SU(3)_R$.

The introduction of the mirror fields enables us to write the mixing terms as

$$\begin{aligned} \mathcal{L}_{m_0} = & -m_0^\psi \text{tr}(\bar{\psi}_R \psi_L^{\text{mir}} - \bar{\psi}_L \psi_R^{\text{mir}}) + \text{H.c.} \\ & -m_0^\chi \text{tr}(\bar{\chi}_R \chi_L^{\text{mir}} - \bar{\chi}_L \chi_R^{\text{mir}}) + \text{H.c.} \\ & -m_0^\eta \text{tr}(\bar{\eta}_R \eta_L^{\text{mir}} - \bar{\eta}_L \eta_R^{\text{mir}}) + \text{H.c.} \end{aligned} \quad (16)$$

The parameter $m_0^{\psi,\chi,\eta}$ corresponds to the chiral-invariant masses of the ψ , χ , and η fields, respectively. Note here that the ψ and χ fields contain flavor-antisymmetric diquarks which are called good diquarks, while the η field contains flavor-symmetric diquark are called bad diquarks. We assume that baryons in representations including ‘‘good’’ diquarks are lighter than those including ‘‘bad’’ diquarks, so the chiral-invariant mass for each baryon field should follow $m_0^\eta \gtrsim m_0^\psi \sim m_0^\chi$. For simplicity, in this paper, we set $m_0^\psi = m_0^\chi$.

III. QUARK DIAGRAM FOR YUKAWA INTERACTION

In this section we study the mass spectra of octet baryons in a model with first-order Yukawa interactions. The Yukawa interaction contains the coupling to the σ fields whose condensation breaks the chiral symmetry. In the standard linear σ model nucleon masses arise from the σ condensate.

For writing the Yukawa interactions, we introduce a 3×3 matrix field M expressing a nonet of scalar and pseudoscalar mesons made of a quark and an antiquark. The representation under $SU(3)_L \times SU(3)_R$ is

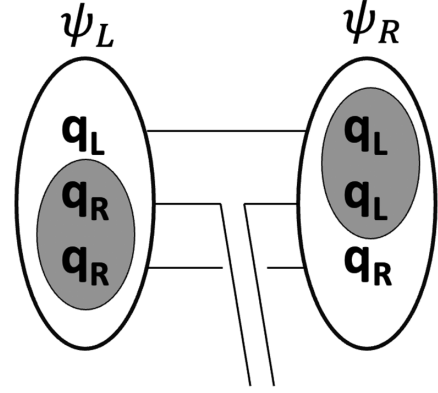


FIG. 2. Yukawa interaction between $(3, \bar{3})$ and $(\bar{3}, 3)$ baryon fields.

$$M \sim (3, \bar{3}). \quad (17)$$

We can then construct the chiral-invariant Yukawa interaction terms at the first order of M for several combinations of $\psi, \psi^{\text{mir}}, \chi, \chi^{\text{mir}}, \eta, \eta^{\text{mir}}$ fields. In the following, we list the possible Yukawa interactions at first order using a way based on the quark diagrams developed in Ref. [40].

We first consider the Yukawa interaction between $(3, \bar{3}) + (\bar{3}, 3)$ representations. We show the corresponding quark diagram in Fig. 2. In this figure, the scalar field M couples to a quark q_R in the good diquark included in the $(3_L, \bar{3}_R)$ representation. After the chiral flipping, the $(\bar{3}_L, 3_R)$ representation is formed. The same is true after exchanges of L and R . We then construct the chiral-invariant term at the first order in M as

$$\begin{aligned} \mathcal{L}^\psi = & g_1 (\epsilon_{abc} \epsilon^{\alpha\beta\sigma} (\bar{\psi}_R)_\alpha^a (M)_\beta^b (\psi_L)_\sigma^c + \text{H.c.}) \\ & + g_2 (\epsilon^{abc} \epsilon_{\alpha\beta\sigma} (\bar{\psi}_R^{\text{mir}})_\alpha^a (M)_b^\beta (\psi_L^{\text{mir}})_c^\sigma + \text{H.c.}), \end{aligned} \quad (18)$$

where the ϵ_{ijk} is the totally antisymmetric tensor.

We next consider the case only with $(3, 6) + (6, 3)$ representation. The corresponding quark diagram is shown in Fig. 3. As shown in this figure, the M field couples to the a quark in the bad diquark included in the $(6_L, 3_R)$ representation, forming another bad diquark in the $(3_L, 6_R)$ representation. The resultant Lagrangian is written as

$$\begin{aligned} \mathcal{L}^\eta = & g_3 ((\bar{\eta}_{1r})_{(ab,a)} (M)_\beta^a (\eta_{1l})^{(b,\alpha\beta)} + \text{H.c.}) \\ & + g_4 ((\bar{\eta}_r^{\text{mir}})_{(a,\alpha\beta)} (M^\dagger)_b^\alpha (\eta_l^{\text{mir}})^{(ab,\beta)} + \text{H.c.}). \end{aligned} \quad (19)$$

For the Yukawa interactions between ψ and η , the matrix M couples to a quark q_L in the good diquark included in the $(\bar{3}_L, 3_R)$ representation. After the chiral flipping the $(3, 6)$ representation is formed as shown in Fig. 4. The chiral-invariant Lagrangian at the leading order in M is constructed as

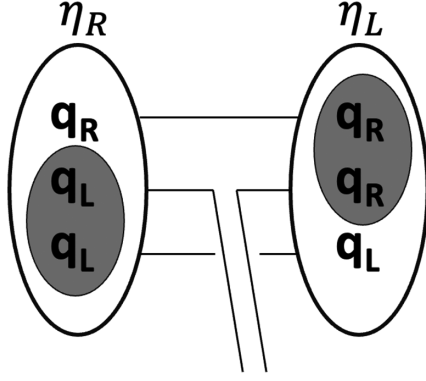


FIG. 3. Yukawa interaction couplings between (3, 6) and (6, 3) baryon fields.

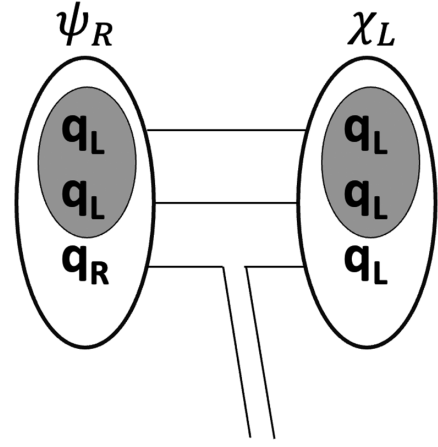
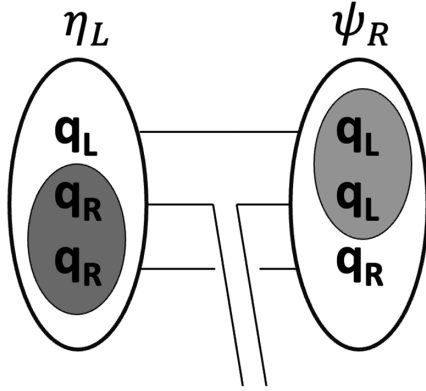
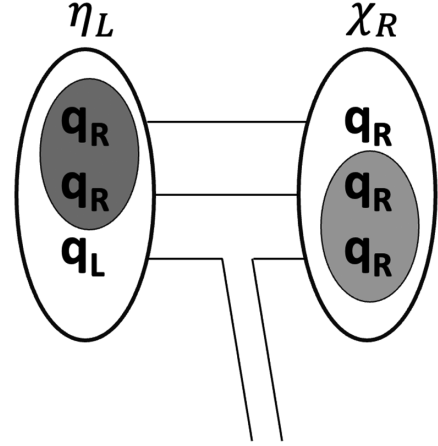

 FIG. 5. Yukawa interaction between $(\bar{3}, 3)$ and (8, 1) baryon fields.

 FIG. 4. Yukawa interaction between (3, 6) and $(\bar{3}, 3)$ baryon fields.


FIG. 6. Yukawa couplings between (3, 6) and (1, 8) baryon fields.

$$\begin{aligned} \mathcal{L}^{\psi\eta} = & y_1 [\epsilon_{abc} (\bar{\psi}_R)_\alpha^a (M)_\beta^b (\eta_L)^{(c,\alpha\beta)} + \text{H.c.}] \\ & + y_3 [\epsilon_{a\beta\sigma} (\bar{\psi}_R^{\text{mir}})_\alpha^a (M)_\beta^b (\eta_L)^{(c,\alpha\beta)} + \text{H.c.}]. \end{aligned} \quad (20)$$

For the Yukawa interactions between ψ and χ , a spectator quark q_L in $(3_L, \bar{3}_R)$ representation couples to M and flips the chirality to form the representation $(1_L, 8_R)$ as shown in Fig. 5. The relevant Lagrangian is written as

$$\begin{aligned} \mathcal{L}^{\psi\chi} = & y_2 \text{tr} (\bar{\psi}_R M^\dagger \chi_L + \text{H.c.}) \\ & + y_4 \text{tr} (\bar{\psi}_R^{\text{mir}} M \chi_L^{\text{mir}} + \text{H.c.}). \end{aligned} \quad (21)$$

Here we have to emphasize that, at the first order in M , there are no Yukawa interactions that couple χ_L and χ_R fields. This is because the χ field contains three valence quarks with all left-handed or right-handed so that Yukawa interactions with χ should include three quark exchanges that flip the chirality of three quarks.

Finally, we consider the Yukawa interaction between $(3_L, 6_R)$ and $(1_L, 8_R)$ representations. The relevant quark diagram is shown in Fig. 6 and the Lagrangian is written as

$$\begin{aligned} \mathcal{L}^{\eta\chi} = & y_5 (\epsilon^{a\sigma\rho} (\bar{\eta}_l)_{(a,\alpha\beta)} (M)_\sigma^a (\chi_r)_\rho^\beta + \text{H.c.}) \\ & + y_6 (\epsilon^{acd} (\bar{\eta}_l^{\text{mir}})_{(ab,\alpha)} (M^\dagger)_c^\alpha (\chi_r^{\text{mir}})_d^b + \text{H.c.}). \end{aligned} \quad (22)$$

Now, the total Lagrangian for the Yukawa interactions at first order in M is expressed as

$$\mathcal{L} = \mathcal{L}^\psi + \mathcal{L}^\eta + \mathcal{L}^{\psi\eta} + \mathcal{L}^{\psi\chi} + \mathcal{L}^{\eta\chi} + \mathcal{L}_{m_0}. \quad (23)$$

We should note that the Lagrangian for the Yukawa interactions completely agrees with the one provided in Ref. [38].

IV. NUMERICAL FITTING

In the previous section, we have constructed the Yukawa interactions at the first order in the scalar M field based on the quark-line diagrams. In this section, we fit the Yukawa couplings to the existing mass spectra of baryons.

We take the mean field approximation in which the meson field M is replaced with its mean field as $\langle M \rangle = \text{diag}(\alpha, \beta, \gamma)$. In the following analysis we assume the isospin symmetry by taking $\alpha = \beta$. It is convenient to introduce a unified notation for the chiral representations of baryons as $\Psi_i = (\psi_i, \eta_i, \chi_i, \gamma_5 \psi_i^{\text{mir}}, \gamma_5 \eta_i^{\text{mir}}, \gamma_5 \chi_i^{\text{mir}})^T$ with $i = N, \Lambda, \Sigma, \Xi$. We then calculate the mass terms of baryons in the form of

$$\mathcal{L} = \sum_{i=N, \Lambda, \Sigma, \Xi} \bar{\Psi}_i \hat{M}_i \Psi_i, \quad (24)$$

where the $\hat{M}_i (i = N, \Lambda, \Sigma, \Xi)$ are the mass matrices for baryons. As an example, the mass matrix for nucleon is

$$M_N = \begin{pmatrix} g_1 \alpha & -\frac{3y_1}{\sqrt{6}} \alpha & -y_2 \alpha & m_0^\psi & 0 & 0 \\ & \frac{g_3}{2} \alpha & -\frac{3y_5}{\sqrt{6}} \alpha & 0 & m_0^\eta & 0 \\ & & 0 & 0 & 0 & m_0^\chi \\ & & & -g_2 \alpha & \frac{3y_3}{\sqrt{6}} \alpha & y_4 \alpha \\ & & & & -\frac{g_4}{2} \alpha & \frac{3y_6}{\sqrt{6}} \alpha \\ & & & & & 0 \end{pmatrix}, \quad (25)$$

where we omit the lower triangular part of the matrix M_N , which is understood from the fact that M_N is the symmetric matrix $(M_N)^T = M_N$.

Diagonalizing this 6×6 matrix \hat{M}_i , we obtain six mass eigenvalues. We focus on the first four states of baryons in this research, as the remaining two states completely come from predictions with large ambiguity. We determine the VEVs of the meson field M from the decay constants of pion and kaon as

TABLE I. Physical inputs of the decay constants for pion and kaon [44], and the VEV of the meson field $\langle M \rangle = \text{diag}\{\alpha, \alpha, \gamma\}$.

f_π	93 MeV
f_K	110 MeV
2α	$f_\pi (= 93 \text{ MeV})$
2γ	$2f_K - f_\pi (= 127 \text{ MeV})$

$$2\alpha = f_\pi, \quad 2\gamma = 2f_K - f_\pi. \quad (26)$$

In Table I, the input values of f_π and f_K are shown together with the determined values of α and γ .

We determine the model parameters based on the following procedure: First we fix chiral-invariant masses, $m^\psi = m^\chi$ and m^η as given and later examine different values of (m^ψ, m^η) . Then we have ten Yukawa couplings $g_{i=1-4}$ and $y_{i=1-6}$ to be used for fitting. Using 12 mass values in Table II as inputs, we determine ten Yukawa coupling constants by minimizing the following error function:

$$f_{\min} = \sum_{i=1}^{12} \left(\frac{m_i^{\text{theory}} - m_i^{\text{input}}}{\delta m_i} \right)^2, \quad (27)$$

where errors δm_i are taken as $\delta m_i = 10 \text{ MeV}$ for the ground-state baryons and $\delta m_i = 100 \text{ MeV}$ for the excited baryons. For the ground-state baryons, the masses are known to high precision, with uncertainties usually less than 1 MeV. Setting $\delta m_i = 10 \text{ MeV}$ for these states ensures that we can well reproduce the ground-state masses after considering the theoretical error. For the excited states, the mass uncertainties are generally larger, ranging from a few MeV to over 100 MeV, depending on the state and the quality of the experimental data. By setting $\delta m_i = 100 \text{ MeV}$ for all excited states, we allow for more flexibility in fitting these masses, reflecting the greater uncertainties in their experimental values.

The 12 baryon states we have chosen are listed in the Particle Data Group (PDG) with reasonable confidence level. The other 12 states not listed in the PDG are the predictions of the present model. For these states we demand the Gell-Mann-Okubo mass relation to the following accuracy:

$$\sum_i |\Delta_{\text{GO},i}| < 100 \text{ MeV}, \quad (28)$$

where

$$\Delta_{\text{GO},i} = \frac{m_i[N] + m_i[\Xi]}{2} - \frac{3m_i[\Lambda] + m_i[\Sigma]}{4}, \quad (29)$$

with i indicating the octet generations as in Table II. This condition reflects the mass difference between up, down,

TABLE II. Physical inputs for the baryon masses belonging to four SU(3)-flavor octets.

J^P	Mass inputs for octet members (MeV)			
	N	Λ	Σ	Ξ
$m_1: 1/2^+$ (ground state)	$N(939): 939$	$\Lambda(1116): 1116$	$\Sigma(1193): 1193$	$\Xi(1318): 1318$
$m_2: 1/2^+$	$N(1440): 1440$	$\Lambda(1600): 1600$	$\Sigma(1660): 1660$	$\Xi(?):$
$m_3: 1/2^-$	$N(1535): 1530$	$\Lambda(1670): 1674$	$\Sigma(1750): 1750$	$\Xi(?):$
$m_4: 1/2^-$	$N(1650): 1650$	$\Lambda(1800): 1800$	$\Sigma(?):$	$\Xi(?):$

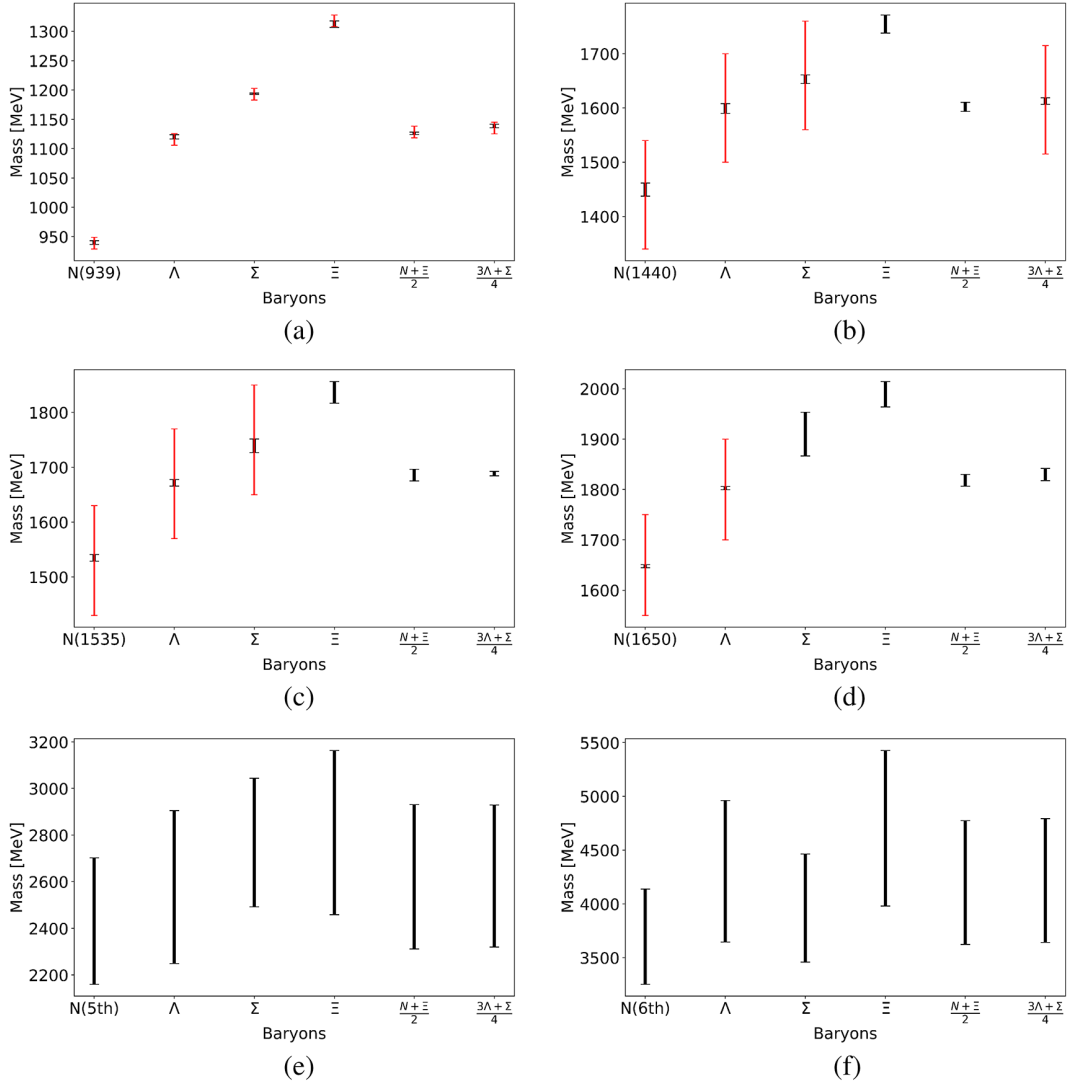


FIG. 7. Masses of octet baryons for the chiral-invariant mass $m_\psi = m_\chi = 700$ MeV and $m_\eta = 1000$ MeV. The red lines show the experimental values with their assigned uncertainties (δm_i), while the black lines show the model predictions for parameter sets satisfying $f_{\min} < 1$, where f_{\min} is the minimum value of the test function f defined in Eq. (27). This condition selects scenarios that reproduce the known baryon masses within an average deviation of 1 standard deviation. (a) Ground state (b) First excited state (c) Second excited state (d) Third excited state (e) Fifth excited state (f) Sixth excited state

and strange quarks and should remain useful even for the mass difference of excited states. The error 100 MeV is chosen to allow for some deviation from the exact Gell-Mann–Okubo relation, considering that our model includes SU(3) symmetry breaking effects and that the baryon masses themselves have uncertainties. The 100 MeV tolerance is a rough estimate of the scale at which we expect these breaking effects to be relevant. We simply reject parameter sets which strongly violate this condition.

In Fig. 7, we show the resultant mass spectrum together with the Gell-Mann–Okubo relation with errors, where the error is determined by requiring $f_{\min}^{\text{best}} < 1$ for $m^\psi = m^\chi = 700$ MeV and $m^\eta = 1000$ MeV. The red line shows the experimental values as inputs. The black line is drawn by

accumulating spectra from all parameter sets satisfying $f_{\min}^{\text{best}} < 1$ and hence reflects the global aspect of our analyses. We find that all the baryon masses below 2 GeV are reproduced well. We emphasize that such a good fit was not possible in the previous research in Ref. [40], where the $(3, \bar{3}) + (\bar{3}, 3)$ and $(8, 1) + (1, 8)$ representations are used to construct a chiral-invariant Lagrangian up to second-order Yukawa interactions, while the $(3, 6) + (6, 3)$ representations are assumed to be integrated out. In particular, the mass hierarchy between Σ and Ξ cannot be correctly reproduced, indicating that the baryon dynamics is not well saturated by just $(3, \bar{3}) + (\bar{3}, 3)$ and $(8, 1) + (1, 8)$ representations. In contrast, the current analyses manifestly including the $(6, 3) + (3, 6)$

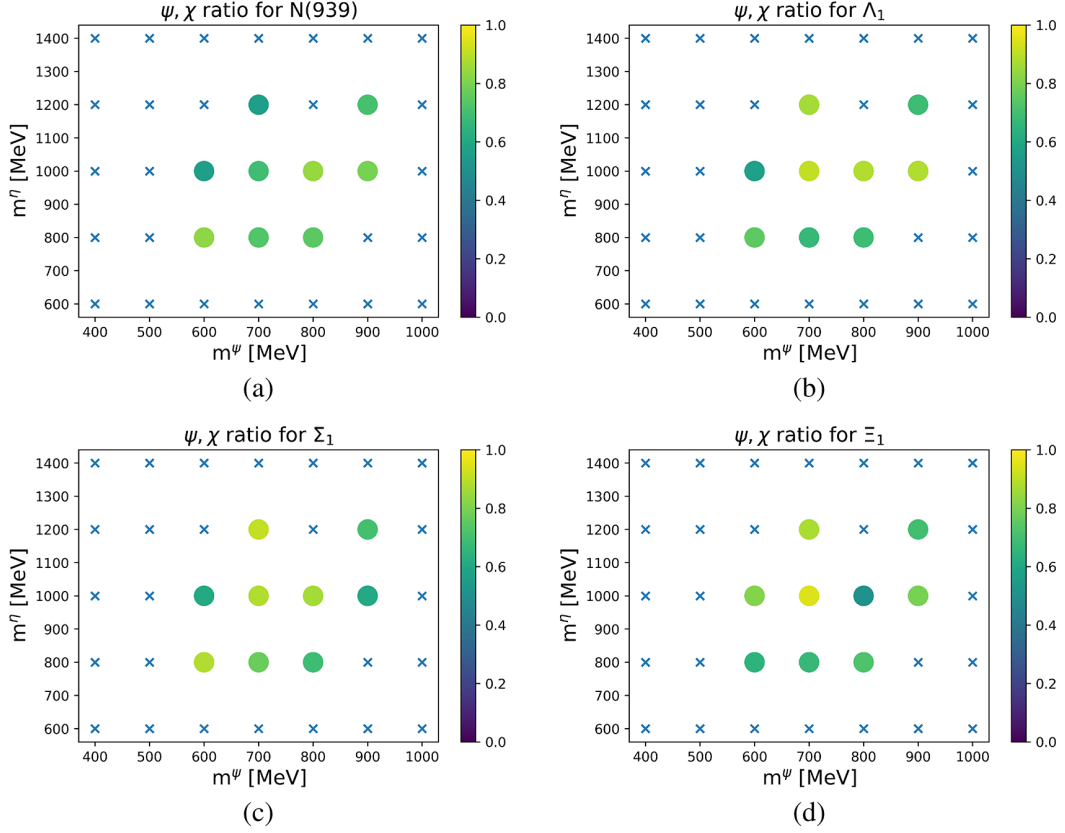


FIG. 8. Numerical results for the probability to find representations with good diquarks, $|c_\psi|^2 + |c_{\psi^{\text{mir}}}|^2 + |c_\chi|^2 + |c_{\chi^{\text{mir}}}|^2$, for each combination of $(m^{\psi(\chi)}, m^\eta)$. (a) Nucleons (b) Λ baryon (c) Σ baryon (d) Ξ baryon.

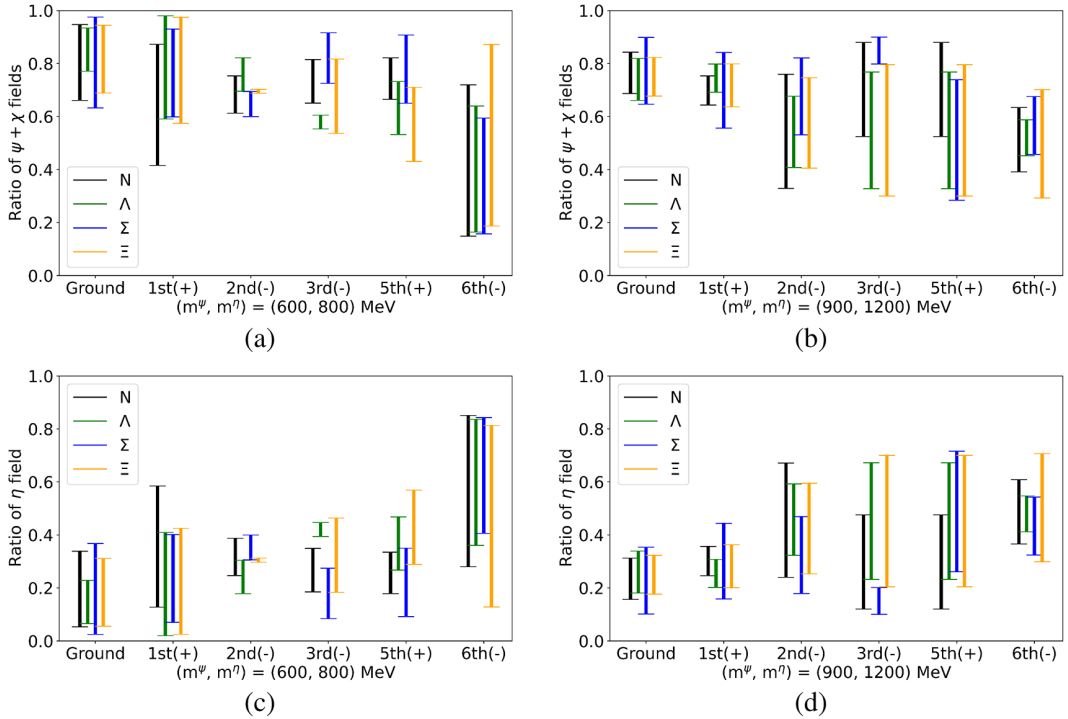


FIG. 9. Numerical results for the probability to find representations with (a), (b) good and (c), (d) bad diquarks, $|c_\psi|^2 + |c_{\psi^{\text{mir}}}|^2 + |c_\chi|^2 + |c_{\chi^{\text{mir}}}|^2$ and $|c_\eta|^2 + |c_{\eta^{\text{mir}}}|^2$, respectively, for a typical choice of $(m^{\psi(\chi)}, m^\eta)$. The sign in the brackets indicates the parity.

representation correctly describe the mass hierarchy between excited Σ and Ξ states. This should be natural simply because the $(6, 3) + (3, 6)$ representations with bad diquarks have more correlations with excited states; attempts to fit excited states without $(6, 3) + (3, 6)$ representations affect fits to the other states, making the previous global analyses problematic. We also make some predictions about the mass of the second excited state of Σ and the excited states of Ξ below 2 GeV.

Next, we examine the composition of each representation for a baryon state. For instance, for a nucleon,

$$|N\rangle = c_\psi|\psi\rangle + c_\chi|\chi\rangle + c_\eta|\eta\rangle + \dots + c_{\eta^{\text{mir}}}|\eta^{\text{mir}}\rangle, \quad (30)$$

where the flavor wave function is normalized to $\langle N|N\rangle = 1$. We examine the probability to find light representations, $|c_\psi|^2 + |c_{\psi^{\text{mir}}}|^2 + |c_\chi|^2 + |c_{\chi^{\text{mir}}}|^2$, in a nucleon. Shown in Fig. 8 in color are the probability to find $|\psi\rangle$ and $|\chi\rangle$ states in the ground states (N , Λ , Σ , Ξ) for given (m^ψ, m^η) . The quality of fit (measured by $f_{\text{min}}^{\text{best}}$) is not always good for some domain of (m_ψ, m_χ) , and such domains with $f_{\text{min}}^{\text{best}} \geq 1$ are marked with crosses and are omitted from our analyses. The best fit for given (m_ψ, m_χ) suggests that the ground states are well dominated by the $(3, \bar{3}) + (\bar{3}, 3)$ and $(8, 1) + (1, 8)$ states including good diquarks.

We also examine how robust the dominance of $(3, \bar{3}) + (\bar{3}, 3)$ and $(8, 1) + (1, 8)$ states is by studying the variance

around the best fit. In Fig. 9, we accumulate the results on composition coming from all the parameter sets satisfying $f_{\text{min}}^{\text{best}} < 1$. The ground to the fifth excited states are displayed for $(m^\psi, m^\eta) = (600, 800)$ MeV and $(900, 1200)$ MeV. The results show that the dominance of $(3, \bar{3}) + (\bar{3}, 3)$ and $(8, 1) + (1, 8)$ states is a robust conclusion. In Fig. 9, we also examine the fraction of the $(6, 3) + (3, 6)$ representation η . The overall tendency is that the fraction gently grows with the excitation levels. These trends are consistent with conventional arguments based on diquark classifications in the hadron spectroscopy.

V. SUMMARY AND DISCUSSION

In this work, we constructed an $SU(3)_L \times SU(3)_R$ invariant parity doublet model based on the quark diagram. In our model, the $(3_L, \bar{3}_R) + (\bar{3}_L, 3_R)$, $(3_L, 6_R) + (6_L, 3_R)$, and $(1_L, 8_R) + (8_L, 1_R)$ representations are manifestly included to describe baryon octet states from the ground states to excited states. We used χ^2 fitting to determine ten parameters in our model to 12 physical inputs and calculated the mass spectra for hyperons with masses smaller than 2 GeV. The mass spectra are well reproduced, as shown in Fig. 7. Also, we obtained the mixing ratio for different representations. For the ground state, the results show that, for all the reasonable combinations of (m^ψ, m^η) , the ψ and χ fields are dominant, indicating the fact that the ground state is well saturated by $(3, \bar{3}) + (\bar{3}, 3)$ and

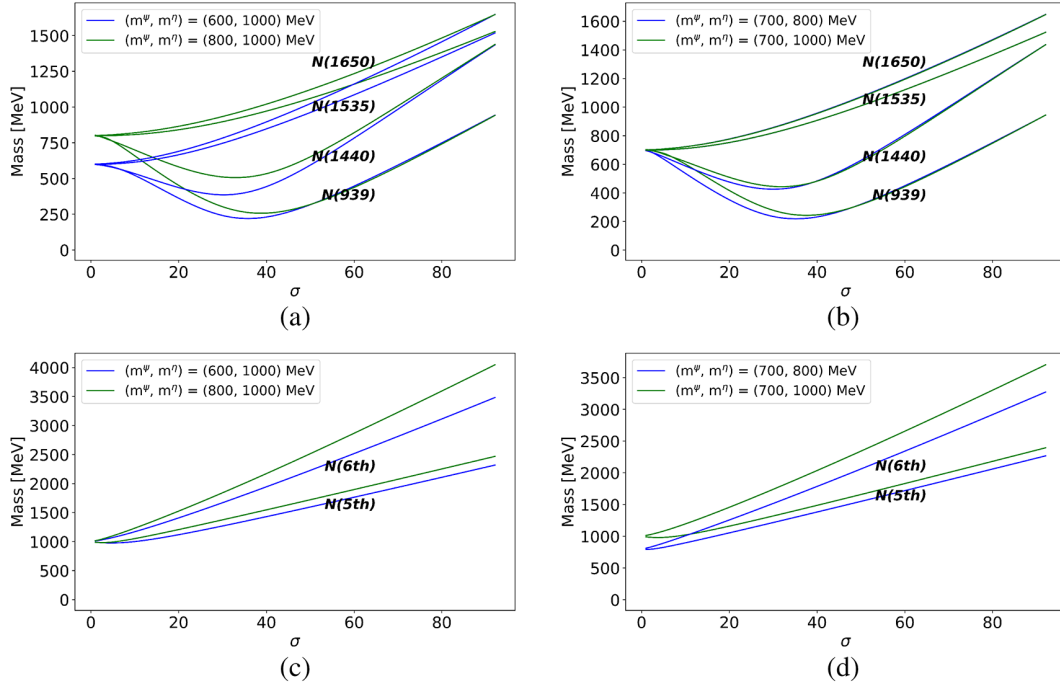


FIG. 10. Numerical results of σ dependence of nucleon mass for each combination of $(m^{\psi(\chi)}, m^\eta)$. We choose the best fitted value for each combination of $(m^{\psi(\chi)}, m^\eta)$. (a) Result for the first four states with fixing $m_\eta = 1000$ MeV. (b) Result for the first four states with fixing $m_\psi = 700$ MeV. (c) Result for the fifth and sixth states with fixing $m_\eta = 1000$ MeV. (d) Result for the fifth and sixth states with fixing $m_\psi = 700$ MeV.

TABLE III. σ dependence of nucleon masses at vacuum.

$(m^{\psi(\chi)}, m^n)$ (MeV)	(600, 1000)	(800, 1000)	(700, 800)	(700, 1000)
$ \partial m_N / \partial \sigma $ [G.S]	16.09	16.02	16.04	16.41
$ \partial m_N / \partial \sigma $ [N(1440)]	20.06	19.31	19.55	19.78
$ \partial m_N / \partial \sigma $ [N(1535)]	13.99	12.23	13.16	13.16
$ \partial m_N / \partial \sigma $ [N(1650)]	16.13	13.86	14.89	15.15
$ \partial m_N / \partial \sigma $ [N(5th)]	17.43	17.90	17.21	17.70
$ \partial m_N / \partial \sigma $ [N(6th)]	30.72	37.56	29.59	33.34

(8, 1) + (1, 8) representations. This is consistent with considerations based on diquarks.

Our new model has improved the mass ordering problem in the previous analyses, but unfortunately there arises another problem concerning the strength of the Yukawa couplings. We close this paper by mentioning this problem and call for further studies.

The Yukawa couplings for reasonable fits are found to be large compared to those used in our previous analyses for the two-flavor case. The magnitude of ten Yukawa couplings are $O(10-30)$, and both positive and negative signs are possible. Our experience for two-flavor analyses indicates that the sum and the difference between the Yukawa couplings are responsible for the average and mass splitting of the positive and negative parity nucleons. To explain the mass splitting of ~ 500 MeV, the couplings cannot be too small for any chiral-invariant masses. What we have not understood is why Yukawa couplings in the three-flavor case become larger than the two-flavor case by a few factors.

Our three-flavor model contains more representations than the two-flavor model, and it might be possible that, after diagonalization to get physical baryon spectra, the physical baryons have a smaller Yukawa coupling, because the Yukawa couplings for the original fields have alternating signs. To check this possibility, we estimate the Yukawa coupling between σ and physical nucleons obtained after diagonalization. For this purpose we compute $\partial m_N / \partial \sigma$.

In Fig. 10, we show the σ dependence of nucleon mass for different generations. The value of σ dependence of nucleon mass are listed in Table III. For each combination of $m^{\psi(\chi)}$ and m^n , we choose the best fitted parameters to reproduce the mass spectrum of each nucleon. In Figs. 10(a) and 10(b), we show the σ dependence of the first four states for two sets of $(m^{\psi(\chi)}, m^n)$, (600, 1000), and (800, 1000) MeV. Increasing σ from 0 to f_π , positive parity states show nonmonotonic behavior, while negative

parity states grow monotonically. This behavior is consistent with SU(2) PDM in Ref. [45]. Next, we vary m^ψ with m^n fixed to 1000 MeV [Fig. 10(a)]. For the first four states, increasing m^ψ reduces $\partial m_N / \partial \sigma$ or the Yukawa coupling to σ , since m^ψ explains the majority of m_N . We also varied m^n with m^ψ fixed to 700 MeV [Fig. 10(b)] and found that the first four states are very insensitive to the details of m_η .

For the other two highest excited states, we found the masses increase almost linearly as a function of σ . This seems odd to us, as we expected that the highly excited states would decouple from the chiral symmetry breaking. We guess that the overall mass scale for these states should be discussed in the context of other mechanisms such as stringy excitations seen in the Regge trajectories.

To summarize, our model for $SU(3)_L \times SU(3)_R$ improved the description of mass ordering associated with the flavor difference, but we found that the size of Yukawa couplings are still problematic. It is surprising to us that imposing the $SU(3)_L \times SU(3)_R$ symmetry [not just $SU(3)_V$] introduces, besides many possible baryonic representations, several unexpected issues in constructing a Lagrangian in the linear realization of chiral symmetry. There still seem to be some missing elements, and we leave those problems for future study.

ACKNOWLEDGMENTS

B. G. is supported by JST SPRING Grant No. JPMJSP2125. B. G. would like to take this opportunity to thank the Interdisciplinary Frontier Next-Generation Researcher Program of the Tokai Higher Education and Research System. M. H. is supported by JSPS KAKENHI Grants No. JP20K03927 and No. JP23H05439. T. K. is supported by JSPS KAKENHI Grants No. 23K03377 and No. 18H05407, and also by the Graduate Program on Physics for the Universe (GPPU) at Tohoku University.

- [1] S. Weinberg, Pion scattering lengths, *Phys. Rev. Lett.* **17**, 616 (1966).
- [2] S. Weinberg, Algebraic realizations of chiral symmetry, *Phys. Rev.* **177**, 2604 (1969).
- [3] S. Weinberg, Mended symmetries, *Phys. Rev. Lett.* **65**, 1177 (1990).
- [4] S. Weinberg, Pions in large- N quantum chromodynamics, *Phys. Rev. Lett.* **105**, 261601 (2010).
- [5] Y. Nambu and G. Jona-Lasinio, Dynamical model of elementary particles based on an analogy with superconductivity. I, *Phys. Rev.* **122**, 345 (1961).
- [6] Y. Nambu and G. Jona-Lasinio, Dynamical model of elementary particles based on an analogy with superconductivity. II, *Phys. Rev.* **124**, 246 (1961).
- [7] T. Hatsuda and T. Kunihiro, QCD phenomenology based on a chiral effective Lagrangian, *Phys. Rep.* **247**, 221 (1994).
- [8] G. Aarts, C. Allton, S. Hands, B. Jäger, C. Praki, and J.-I. Skullerud, Nucleons and parity doubling across the deconfinement transition, *Phys. Rev. D* **92**, 014503 (2015).
- [9] G. Aarts, C. Allton, D. De Boni, S. Hands, B. Jäger, C. Praki, and J.-I. Skullerud, Light baryons below and above the deconfinement transition: Medium effects and parity doubling, *J. High Energy Phys.* **06** (2017) 034.
- [10] G. Aarts, C. Allton, D. de Boni, S. Hands, B. Jäger, C. Praki, and J.-I. Skullerud, Baryons in the plasma: In-medium effects and parity doubling, *EPJ Web Conf.* **171**, 14005 (2018).
- [11] G. Aarts, C. Allton, D. De Boni, and B. Jäger, Hyperons in thermal QCD: A lattice view, *Phys. Rev. D* **99**, 074503 (2019).
- [12] G. Aarts, C. Allton, D. de Boni, J. Glesaaen, S. Hands, B. Jäger, and J.-I. Skullerud, *Hyperons in Thermal QCD from the Lattice*, Springer Proceedings in Physics Vol. 250 (Springer, New York, 2020), pp. 29–35.
- [13] C. E. Detar and T. Kunihiro, Linear σ model with parity doubling, *Phys. Rev. D* **39**, 2805 (1989).
- [14] D. Jido, Y. Nemoto, M. Oka, and A. Hosaka, Chiral symmetry for positive and negative parity nucleons, *Nucl. Phys. A* **671**, 471 (2000).
- [15] D. Jido, T. Hatsuda, and T. Kunihiro, Chiral symmetry realization for even parity and odd parity baryon resonances, *Phys. Rev. Lett.* **84**, 3252 (2000).
- [16] D. Jido, M. Oka, and A. Hosaka, Chiral symmetry of baryons, *Prog. Theor. Phys.* **106**, 873 (2001).
- [17] K. Nagata, A. Hosaka, and V. Dmitrasinovic, πN and $\pi\pi N$ couplings of the $\Delta(1232)$ and its chiral partners, *Phys. Rev. Lett.* **101**, 092001 (2008).
- [18] S. Gallas, F. Giacosa, and D. H. Rischke, Vacuum phenomenology of the chiral partner of the nucleon in a linear sigma model with vector mesons, *Phys. Rev. D* **82**, 014004 (2010).
- [19] S. Gallas and F. Giacosa, Mirror versus naive assignment in chiral models for the nucleon, *Int. J. Mod. Phys. A* **29**, 1450098 (2014).
- [20] Y. Motohiro, Y. Kim, and M. Harada, Asymmetric nuclear matter in a parity doublet model with hidden local symmetry, *Phys. Rev. C* **92**, 025201 (2015); *Phys. Rev. C* **95**, 059903(E) (2017).
- [21] C. Sasaki and I. Mishustin, Thermodynamics of dense hadronic matter in a parity doublet model, *Phys. Rev. C* **82**, 035204 (2010).
- [22] J. Eser and J.-P. Blaizot, Thermodynamics of the parity-doublet model: Symmetric nuclear matter and the chiral transition, *Phys. Rev. C* **109**, 045201 (2024).
- [23] T. Yamazaki and M. Harada, Constraint to chiral invariant masses of nucleons from GW170817 in an extended parity doublet model, *Phys. Rev. C* **100**, 025205 (2019).
- [24] G. Baym, T. Hatsuda, T. Kojo, P. D. Powell, Y. Song, and T. Takatsuka, From hadrons to quarks in neutron stars: A review, *Rep. Prog. Phys.* **81**, 056902 (2018).
- [25] T. Minamikawa, T. Kojo, and M. Harada, Quark-hadron crossover equations of state for neutron stars: Constraining the chiral invariant mass in a parity doublet model, *Phys. Rev. C* **103**, 045205 (2021).
- [26] T. Minamikawa, T. Kojo, and M. Harada, Chiral condensates for neutron stars in hadron-quark crossover: From a parity doublet nucleon model to a Nambu–Jona-Lasinio quark model, *Phys. Rev. C* **104**, 065201 (2021).
- [27] B. Gao, T. Minamikawa, T. Kojo, and M. Harada, Impacts of the U(1)A anomaly on nuclear and neutron star equation of state based on a parity doublet model, *Phys. Rev. C* **106**, 065205 (2022).
- [28] T. Minamikawa, B. Gao, T. Kojo, and M. Harada, Chiral restoration of nucleons in neutron star matter: Studies based on a parity doublet model, *Symmetry* **15**, 745 (2023).
- [29] M. Marczenko, D. Blaschke, K. Redlich, and C. Sasaki, Parity doubling and the dense matter phase diagram under constraints from multi-messenger astronomy, *Universe* **5**, 180 (2019).
- [30] B. P. Abbott (LIGO Scientific and Virgo Collaborations), GW170817: Observation of gravitational waves from a binary neutron star inspiral, *Phys. Rev. Lett.* **119**, 161101 (2017).
- [31] B. P. Abbott *et al.* (LIGO Scientific, Virgo, Fermi GBM, INTEGRAL, IceCube, AstroSat Cadmium Zinc Telluride Imager Team, IPN, Insight-Hxmt, ANTARES, Swift, AGILE Team, 1M2H Team, Dark Energy Camera GW-EM, DES, DLT40, GRAWITA, Fermi-LAT, ATCA, ASKAP, Las Cumbres Observatory Group, OzGrav, DWF (Deeper Wider Faster Program), AST3, CAASTRO, VINROUGE, MASTER, J-GEM, GROWTH, JAGWAR, CaltechNRAO, TTU-NRAO, NuSTAR, Pan-STARRS, MAXI Team, TZAC Consortium, KU, Nordic Optical Telescope, ePESSTO, GROND, Texas Tech University, SALT Group, TOROS, BOOTES, MWA, CALET, IKI-GW Follow-up, H.E.S.S., LOFAR, LWA, HAWC, Pierre Auger, ALMA, Euro VLBI Team, Pi of Sky, Chandra Team at McGill University, DFN, ATLAS Telescopes, High Time Resolution Universe Survey, RIMAS, RATIR, and SKA South Africa/MeerKAT Collaborations), Multi-messenger observations of a binary neutron star merger, *Astrophys. J. Lett.* **848**, L12 (2017).
- [32] B. P. Abbott *et al.* (LIGO Scientific and Virgo Collaborations), GW170817: Measurements of neutron star radii and equation of state, *Phys. Rev. Lett.* **121**, 161101 (2018).
- [33] T. E. Riley *et al.*, A NICER view of the massive pulsar PSR J0740 + 6620 informed by radio timing and XMM-Newton spectroscopy, *Astrophys. J. Lett.* **918**, L27 (2021).
- [34] M. C. Miller *et al.*, The radius of PSR J0740 + 6620 from NICER and XMM-Newton data, *Astrophys. J. Lett.* **918**, L28 (2021).

- [35] H.-X. Chen, V. Dmitrasinovic, and A. Hosaka, Baryon fields with $U_L(3) \times U_R(3)$ chiral symmetry II: Axial currents of nucleons and hyperons, *Phys. Rev. D* **81**, 054002 (2010).
- [36] H.-X. Chen, V. Dmitrasinovic, and A. Hosaka, Baryon fields with $U_L(3) \times U_R(3)$ chiral symmetry III: Interactions with chiral $(3, \bar{3}) + (\bar{3}, 3)$ spinless mesons, *Phys. Rev. D* **83**, 014015 (2011).
- [37] H.-X. Chen, V. Dmitrasinovic, and A. Hosaka, Baryons with $U_L(3) \times U_R(3)$ chiral symmetry IV: Interactions with chiral $(8, 1) \oplus (1, 8)$ vector and axial-vector mesons and anomalous magnetic moments, *Phys. Rev. C* **85**, 055205 (2012).
- [38] H. Nishihara and M. Harada, Extended Goldberger-Treiman relation in a three-flavor parity doublet model, *Phys. Rev. D* **92**, 054022 (2015).
- [39] V. Dmitrašinović, H.-X. Chen, and A. Hosaka, Baryon fields with $U_L(3) \times U_R(3)$ chiral symmetry. V. Pion-nucleon and kaon-nucleon Σ terms, *Phys. Rev. C* **93**, 065208 (2016).
- [40] T. Minamikawa, B. Gao, T. Kojo, and M. Harada, Parity doublet model for baryon octets: Diquark classifications and mass hierarchy based on the quark-line diagram, *Phys. Rev. D* **108**, 076017 (2023).
- [41] E. S. Fraga, R. da Mata, and J. Schaffner-Bielich, SU(3) parity doubling in cold neutron star matter, *Phys. Rev. D* **108**, 116003 (2023).
- [42] P. Papazoglou, S. Schramm, J. Schaffner-Bielich, H. Stoecker, and W. Greiner, Chiral Lagrangian for strange hadronic matter, *Phys. Rev. C* **57**, 2576 (1998).
- [43] J. Schechter, Y. Ueda, and G. Venturi, K^+ -nucleon scattering in an effective chiral Lagrangian model, *Phys. Rev.* **177**, 2311 (1969).
- [44] R. L. Workman *et al.* (Particle Data Group), Review of particle physics, *Prog. Theor. Exp. Phys.* **2022**, 083C01 (2022).
- [45] M. Marczenko, K. Redlich, and C. Sasaki, Fluctuations near the liquid-gas and chiral phase transitions in hadronic matter, *Phys. Rev. D* **107**, 054046 (2023).